

UDC 541.49:548.736:544.142.4

STERIC EFFECT ON CONSTRUCTION OF EXTENDED ARCHITECTURES OF Ni(II) COMPLEXES DIRECTED BY INTERMOLECULAR C—H···F AND C—H···O INTERACTIONS© 2010 **H. Kwak¹, G.H. Eom¹, S.H. Lee¹, H.G. Koo¹, S.P. Jang¹, J. Lee², W. Shin², M.S. Lah³, C. Kim^{1*}, S.-J. Kim^{4*}, Y. Kim⁴**¹*Department of Fine Chemistry, and Eco-Product and Materials Education Center, Seoul National University of Technology, Seoul 139-743, Korea*²*Department of Chemistry and Interdisciplinary Program of Integrated Biotechnology, Sogang University, Seoul 121-742, Korea*³*Department of Applied Chemistry, College of Science, Hanyang University, Ansan-si, Gyeonggi-do 426-791, Korea*⁴*Department of Chemistry and Nano Science, Ewha Womans University, Seoul 120-750, Korea**Received January, 22, 2009*

Five new Ni(II) complexes with pyridine carboxamide ligands have been synthesized and the crystal structures of three of the complexes were determined. Strong distortion effects of 6-methyl substitution were observed in the complexes with 6-methyl-substituted pyridyl bpb ligands. The C—H···F and C—H···O hydrogen bond interactions build extended architectures in the crystals studied. This result suggests that the steric effect of 6-methyl substitution plays an important role in the distortion of the structure, and the 6-methyl substitution can facilitate hydrogen bond interactions between methyl hydrogen atoms and O(carbonyl) or F atoms. Twelve Ni(II) complexes, including seven complexes reported previously, show reversible redox behavior, implying that the reduced Ni(I) state of each complex is stable in the time scale of CV measurement. The steric effect of R₁ substituent and the electronic effects of X₁ and X₂ groups were found to be the main factors contributing to the shift of the redox potential of the Ni(II) complexes.

Keywords: Pyridine carboxamide, nickel(II) complex, crystal structure, electronic effect, weak interactions, hydrogen bond, supramolecular architecture, cyclic voltammetry.

Deprotonation of the carboxamide nitrogen atoms in the pyridine carboxamide type ligand bpb (Scheme 1) makes it a tetradentate ligand that chelates metal ions to form a planar geometry complex [1–6]. In this planar geometry, hydrogen atoms in the pyridyl 6'-position make close intramolecular contacts. If methyl groups are placed in the pyridyl 6'-position, they yield highly distorted geometries [7]. The steric effect of 6-methyl substitution in the crystal structures of Cu(II) complexes have been studied and it was shown that 6-methyl substitution can facilitate the formation of extended structures due to interactions between Cu(II) ions and carbonyl oxygen atoms of neighboring molecules [7]. Among analogous nickel complexes containing pyridine carboxamide type ligands, the compound **3** ([Ni(bpb)], see Scheme 1 for the structure) shows almost planar molecular arrangement, while the compound **9** ([Ni(6-Me₂-bpb)]) is a complex that shows the steric effect [8].

These simple Ni(II) complex units can be used as building blocks to form extended structures by the non-classical C—H···O or C—H···F hydrogen bond interactions [7]. It is known that the non-classical interactions can provide good structural motifs for construction of extended architectures and

* E-mail: chealkim@snut.ac.kr; sjkim@ewha.ac.kr

stabilize the crystal structures [10–18]. We have recently reported that in Pd(II) complexes containing both C—X (X = F or Cl) and C=O hydrogen bond accepting sites, the C—F and C—Cl sites can compete with C=O to form hydrogen bond interactions [19].

In order (1) to systematically investigate such a steric effect of a substituent at 6'-position on construction of Ni(II) complexes and their voltammetric behaviors, and (2) to study the role of C—H···F and C—H···O interactions in the formation of the extended structures, two new ligands containing —CH₃ on the pyridyl 6'-position [H₂6-Me₂-bpCl₂ (**L11**) and H₂6-Me₂-bpn (**L12**)] and five new nickel(II) complexes were synthesized. Here we report crystal structures of three new Ni(II) complexes (**7**, **10** and **12**) with pyridine carboxamide ligands (**L7**, **L10** and **L12**), and discuss the steric effect of 6-methyl substitution for nickel complexes with/without 6-methyl groups. In addition, the voltammetric studies of the Ni(II) complexes are reported to exhibit reversible redox behavior which shows that the reduced Ni(I) state of each complex is stable in the timescale of CV (cyclic voltammetry) measurements. The introduction of CH₃ instead of H in R₁ position made the reduction of the complex easier, and the substituent effect of X₁ and X₂ groups on the potential shift was observed. The steric effect of R₁ and the electronic effects of X₁ and X₂ are major contributors to the voltammetric behavior of the Ni(II) complexes studied.

EXPERIMENTAL

Ligands. Ligands **L1**—**L10** were available from a previous study [9, 19–24]. Ligands **L11** (H₂6-Me₂-bpCl₂) and **L12** (H₂6-Me₂-bpn) were prepared by the reactions of appropriate diamines (10 mmol) with 6-methyl-2-picolinic acid (20 mmol) in pyridine in the presence of triphenylphosphite (20 mmol) according to a literature method [19]. For **L11**, the yield was 2.08 g (50.0 %). ¹H NMR (CDCl₃, 300 MHz): δ 2.46 (s, 6H, 2CH₃), δ 7.32–8.11 (m, 8H, aromatic-H), 10.34 (s, 2H, 2N—H). IR (KBr): (N—H) 3274 and (C=O) 1688 cm⁻¹. Anal. Calcd for C₂₀H₁₄N₄O₂Cl₂ (413.28): C, 58.12; H, 3.42; N, 13.56. Found: C, 58.23; H, 3.31; N, 13.27. For **L12**, the yield was 1.76 g (45.2 %). ¹H NMR (DMSO-*d*₆, 300MHz): δ 2.62 (s, 6H, 2CH₃), 6.65–8.80 (m, 9H, aromatic-H), 10.10 (s, 1H, N—H), 11.05 (s, 1H, N—H). IR (KBr): (N—H) 3253 and 3330 and (C=O) 1669 and 1700 cm⁻¹. Anal. Calcd for C₂₀H₁₅N₅O₄ (389.4): C, 61.68; H, 3.89; N, 17.99. Found: C, 61.92; H, 4.01; N, 17.57.

Complexes. Complexes **1**—**6** were available from a previous study [9]. Complexes **7**—**12** were prepared by the reaction of a corresponding ligand (0.5 mmol) with nickel(II) acetate (0.5 mmol) in CH₃CN (20 mL) in good yields, according to a literature method [8, 9]. Crystals of the complexes **7**, **10** and **12** were grown by slow evaporation of the corresponding solutions in EtOH/ether for **7**, CH₃CN/ether for **10**, and CHCl₃/benzene for **12**. For **7**, the yield was 0.11 g (48.3 %). ¹H NMR (CDCl₃, 300 MHz): δ 2.31 (s, 6H, 2CH₃), δ 2.74 (s, 6H, 2CH₃), δ 7.27–7.85 (m, 8H, aromatic-H). IR (KBr): (C=O) 1633 cm⁻¹. Anal. Calcd for C₂₂H₂₀N₄NiO₂ (431.13): C, 61.29; H, 4.69; N, 13.00. Found: C, 60.82; H, 5.10; N, 12.76. For **8**, the yield was 0.10 g (50.0 %). ¹H NMR (CDCl₃, 300MHz): δ 2.27 (s, 3H, CH₃), δ 2.37 (s, 6H, 2CH₃), δ 6.66–8.01 (m, 9H, aromatic-H). IR (KBr): (C=O) 1634 cm⁻¹. Anal. Calcd for C₂₁H₁₈N₄NiO₂ (417.12): C, 60.46; H, 4.36; N, 13.43. Found: C, 60.13; H, 4.11; N, 13.72. Complex **9** was synthesized according to a literature method and its crystal structure has been already reported [8]. The yield was 0.11 g (55.1 %). ¹H NMR (CDCl₃, 300MHz): δ 2.37 (s, 6H, 2CH₃), 6.85–8.12 (m, 10H, aromatic-H). IR (KBr): (C=O) 1637 cm⁻¹. Anal. Calcd for C₂₀H₁₆N₄NiO₂ (403.09): C, 59.59; H, 4.00; N, 13.90. Found: C, 59.50; H, 3.67; N, 14.24. For **10**, the yield was 0.10 g (49.8 %). ¹H NMR (CDCl₃, 300 MHz): δ 2.38 (s, 6H, 2CH₃), 6.54–8.07 (m, 9H, aromatic-H). IR (KBr): (C=O) 1634 cm⁻¹. Anal. Calcd for C₂₀H₁₅FN₄NiO₂ (421.07): C, 57.05; H, 3.60; N, 13.31. Found: C, 57.37; H, 3.55; N, 12.97. For **11**, the yield was 0.16 g (66.5 %). ¹H NMR (CDCl₃, 300 MHz): δ 2.39 (s, 6H, 2CH₃), 7.00–8.25 (m, 8H, aromatic-H). IR (KBr): (C=O) 1644 cm⁻¹. Anal. Calcd for C₂₀H₁₄N₄NiO₂Cl₂ (471.97): C, 50.89; H, 3.00; N, 11.87. Found: C, 51.21; H, 3.05; N, 11.52. For **12**, the yield was 0.14 g (65.3 %). ¹H NMR (DMSO-*d*₆, 300MHz): δ 2.72 (s, 6H, 2CH₃), 6.57–8.28 (m, 9H, aromatic-H). IR (KBr): (C=O) 1650 cm⁻¹. Anal. Calcd for C₂₃H₁₈N₅NiO₄ (487.13): C, 56.71; H, 3.73; N, 14.38. Found: C, 56.54; H, 3.98; N, 14.27.

Table 1

Crystallographic data and refinement details for compounds **7**, **10** and **12**

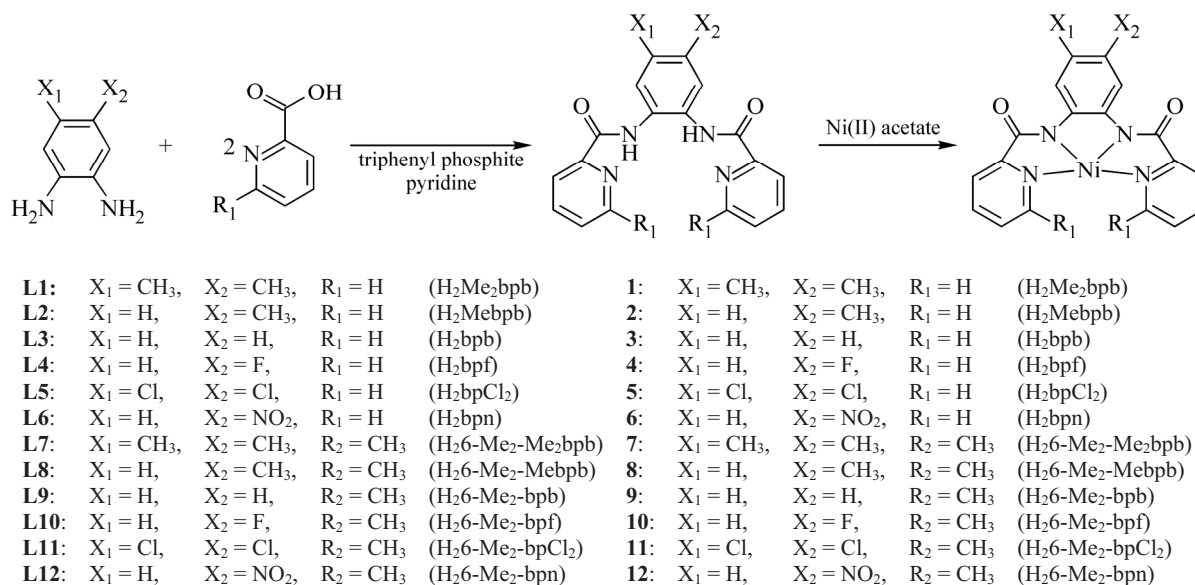
Compound	[Ni(6-Me ₂ -Me ₂ bpb)] (7)	[Ni(6-Me ₂ -bpf)] (10)	[Ni(6-Me ₂ -NO ₂ bpb)] (12)
Empirical formula	C ₂₂ H ₂₀ N ₄ NiO ₂	C ₂₀ H ₁₅ FN ₄ NiO ₂	C ₂₃ H ₁₈ N ₅ NiO ₄
<i>M</i>	431.13	421.07	487.13
<i>T</i> , K	293(2)	293(2)	170(2)
Space group	<i>C</i> 2/ <i>c</i>	P-1	<i>C</i> 2/ <i>c</i>
<i>a</i> , <i>b</i> , <i>c</i> , Å	11.902(2), 24.955(5), 7.1446(14)	8.012(4), 10.493(5), 11.663(5)	26.461(5), 7.0270(12), 23.628(4)
α , β , γ , deg.	90, 91.17(3), 90	106.969(7), 97.485(7), 95.006(7)	90, 113.087(3), 90
<i>V</i> , Å ³	1977.1(7)	921.7(7)	4041.5(12)
<i>Z</i>	4	2	8
<i>d</i> (calc.), g/cm ³	1.448	1.517	1.601
Absorption coeff., mm ⁻¹	1.007	1.086	1.004
Crystal size, mm	0.20×0.15×0.15	0.20×0.15×0.15	0.28×0.28×0.08
Reflections collected	2016	6451	10945
Independent reflections [<i>R</i> (int)]	1918 [0.0173]	3154 [0.0167]	4653 [0.0528]
Refined parameters	134	260	338
GOOF on <i>F</i> ²	1.092	1.068	1.070
<i>R</i> indices [<i>I</i> > 2σ(<i>I</i>)]	<i>R</i> 1 = 0.0456, <i>wR</i> 2 = 0.1312	<i>R</i> 1 = 0.0595, <i>wR</i> 2 = 0.1644	<i>R</i> 1 = 0.0641, <i>wR</i> 2 = 0.1342
<i>R</i> indices (all data)	<i>R</i> 1 = 0.0571, <i>wR</i> 2 = 0.1387	<i>R</i> 1 = 0.0620, <i>wR</i> 2 = 0.1679	<i>R</i> 1 = 0.1156, <i>wR</i> 2 = 0.1527
CCDC deposition <i>N</i>	704020	704021	704022

Crystallography. The diffraction data for the compound [Ni(6-Me₂-Me₂bpb)] (**7**) were collected on an Enraf-Nonius CAD-4 diffractometer equipped with a monochromated MoK_α (λ = 0.71073 Å) radiation source. The crystal was mounted on a glass fiber. The final unit cell parameters were obtained from a least squares refinement of 25 reflections in the range 9.46 ≤ θ ≤ 12.47°. The crystal structure was determined by direct methods and Fourier technique. All the calculations were performed on IBM Pentium computer using SHELXS-97 [25] and SHELXL-97 [26]. All hydrogen atoms were placed in calculated positions. The diffraction data for the compounds [Ni(6-Me₂-bpf)] (**10**) and [Ni(6-Me₂-bpn)] (**12**) were collected on a Bruker SMART APEX diffractometer with MoK_α (λ = 0.71073 Å) radiation source and CCD detector. The crystals were mounted on glass fibers with epoxy glue. The data were integrated and scaled using SAINT; the structures were solved and refined using SHELXTL [27]. Hydrogen atoms were placed in calculated positions. A summary of crystallographic data for compounds **7**, **10** and **12** is given in Table 1.

Full crystallographic information for the compounds **7**, **10** and **12** studied in this work was deposited with CCDC with deposition numbers 704020, 704021 and 704022, respectively. Copies of the data are available free of charge from <http://www.ccdc.cam.ac.uk>.

RESULTS AND DISCUSSION

Syntheses. The synthesis of bpb type ligands and their corresponding Ni(II) complexes is summarized in Scheme 1. Ligands **L11** and **L12** were prepared in moderate yields (40–60 %). The complexes **7–12** were obtained from the reaction of each ligand with nickel(II) acetate hexahydrate in CH₃CN in good yields (50–70 %). The complexes **7–12** (with 6-methyl) were isolated as yellow solids well soluble in DMSO and DMF. Crystals of the complexes **7**, **10** and **12** were grown by slow evaporation of their solutions in appropriate solvent systems as explained in Experimental Section. All the complexes were stable in air.



Scheme 1. Syntheses of ligands and their Ni(II) complexes

Crystal structures. The structures of [Ni(Me₂bpb)] (**1**), [Ni(bpf)] (**4**) and [Ni(bpn)] (**6**) reported previously [9] are similar to that of [Ni(bpb)] (**3**) and have a planar molecular arrangement [8]. Reported in this paper three new Ni(II) complexes [Ni(6-Me₂-Me₂bpb)] (**7**), [Ni(6-Me₂-bpf)] (**10**) and [Ni(6-Me₂-bpn)] (**12**) contain 6-methyl-substituted pyridyl bpb ligands (**L7**, **L10** and **L12**). The X₁X₂R₁-bpb²⁻ ligands coordinate to Ni(II) ions to form monomeric complex units, while C—H···F and C—H···O hydrogen bond interactions extend them to architectures of a higher dimensionality. IR spectroscopy confirmed the deprotonation of the ligands as ν_{NH} bands disappeared, while the ν_{CO} bands shifted to lower wave-number range as compared to those in H₂X₁X₂R₁-bpb (see Experimental Section). Selected bond distances and angles characterizing the coordination are listed in Table 2.

Four N atoms of a corresponding ligand [6-Me₂-Me₂bpb²⁻ (**L7**), 6-Me₂-bpf²⁻ (**L10**) or 6-Me₂-bpn²⁻ (**L12**)] coordinate the Ni(II) ion. The molecular structures of the Ni(II) complexes (**7**, **10** and **12**) are illustrated in Fig. 1. The F atom in compound **10** is disordered over two positions (C9 and C10). The molecule of compound **12** contains two sets of disordered NO₂-benzene rings (Fig. 1, c). The Ni—N(amide) distances of **7**, **10** and **12** are shorter than the Ni—N(pyridyl) distances (Table 2). Two pyridyl rings are considerably tilted, with the dihedral angle of 43.40(9)° for **7**, 42.83(13)° for **10**, and 37.62(11)° for **12**. The distorting effect of methyl substitution is obvious, and the geometry of all three complexes is distorted from that expected for square planar complexes. Similar distortion was demonstrated for the analogous copper(II) complexes [7]; the copper(II) structures showed square pyramidal coordination with interactions between Cu(II) ions and neighboring carbonyl oxygen atoms [7]. In case of the Ni(II) complexes, there are C—H···O and C—H···F interactions to form extended polymeric motifs.

Table 2

Selected bond lengths (Å) and angles (deg.) for compound **7**, **10** and **12**

Parameter	7	10	12
Ni—N(pyridyl)	1.931(2)	1.940(3), 1.959(3)	1.945(4), 1.946(4)
Ni—N(amide)	1.824(2)	1.835(3), 1.836(3)	1.815(5), 1.832(4)
C=O	1.219(4)	1.222(5), 1.235(5)	1.226(6), 1.242(5)
N(amide)—Ni—N(amide)	80.8(2)	83.3(1)—84.3(1)	83.1(2)—84.9(2)
N(pyridyl)—Ni—N(pyridyl)	110.0(1)	110.4(1)	109.8(2)

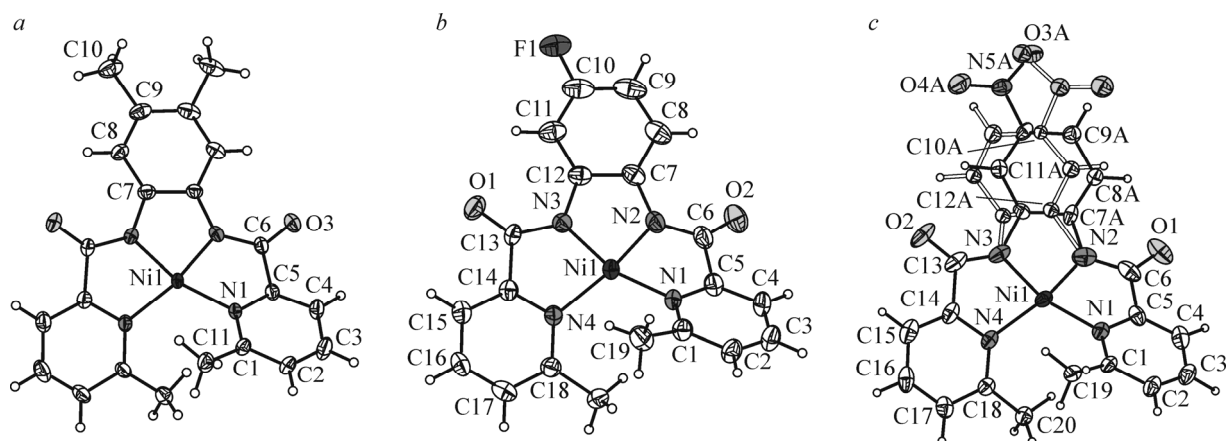


Fig. 1. Molecular structure of complexes **7** (a), **10** (b) and **12** (c). Displacement ellipsoids are shown at the 30 % probability level

The C—H \cdots O or C—H \cdots F hydrogen bond interactions build extended architectures in the Ni(II) complexes containing pyridine carboxamide ligands: compounds **1** and **4** without 6-methyl groups in the pyridine rings and compounds **7**, **10** and **12** with 6-methyl groups. For both compounds **1** (without 6-methyl) and **7** (with 6-methyl) containing the Me₂bpb²⁻ skeleton, different kinds of C—H \cdots O hydrogen bonds generate different types of two-dimensional sheets: a staircase 2D sheet by C(pyridyl)—H \cdots O interactions for **1**, and a 2D sheet by C(methyl)—H \cdots O interactions for **7** (Fig. 2). The presence of 6-methyl group in the pyridyl 6'-positions generates hydrogen bonds between methyl hydrogen atoms and carbonyl oxygen atoms. For both compounds **4** (without 6-methyl) and **10** (with 6-methyl) containing the bpf²⁻ skeleton, the same kinds of hydrogen bonds generate 2D sheets (Fig. 3). Hydrogen bonds between pyridyl hydrogen atoms and carbonyl oxygen atoms or fluorine atoms build the

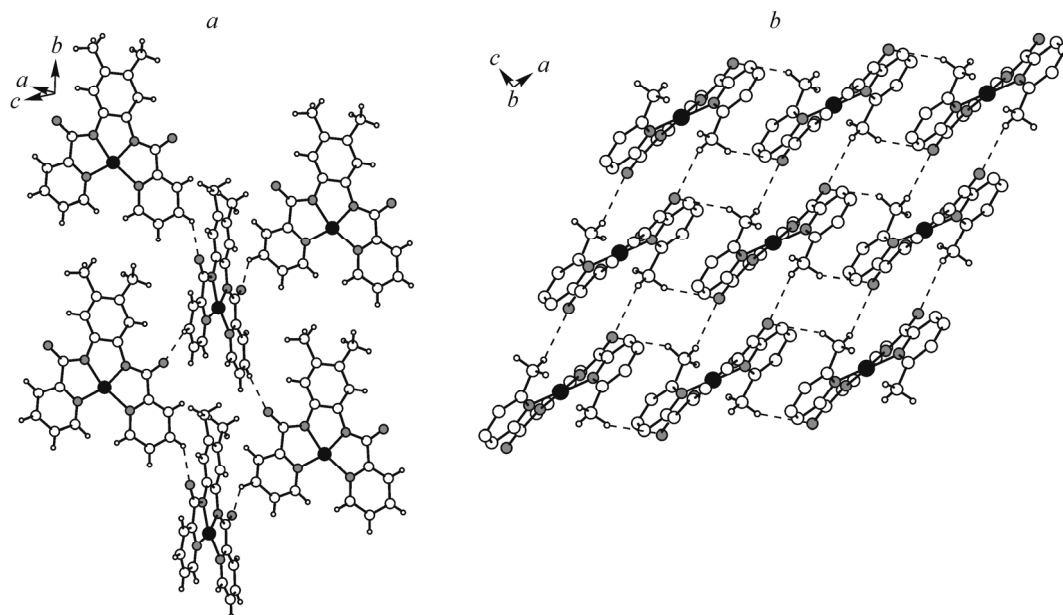


Fig. 2. Two-dimensional sheets built by C(pyridyl)—H \cdots O hydrogen bonds in compound **1** (a) and C(methyl)—H \cdots O hydrogen bonds in compound **7** (b). H atoms not involved in intermolecular interactions have been omitted for clarity. The open dotted lines represent C(methyl)—H \cdots O interactions.

Hydrogen bond C...O lengths [C—H...O angles]: for **1**, C3(pyridyl)—H3A...O1(1.5-x, -0.5+y, z) 2.341(1) Å [133.32(1)°]; for **7**, C11(methyl)—H11A...O3(-0.5-x, 1.5-y, -0.5+z) 2.62(3) Å [124.19(1)°], C11(methyl)—H11B...O3(1.5-x, 1.5-y, 1-z) 2.61(4) Å [139.47(1)°]

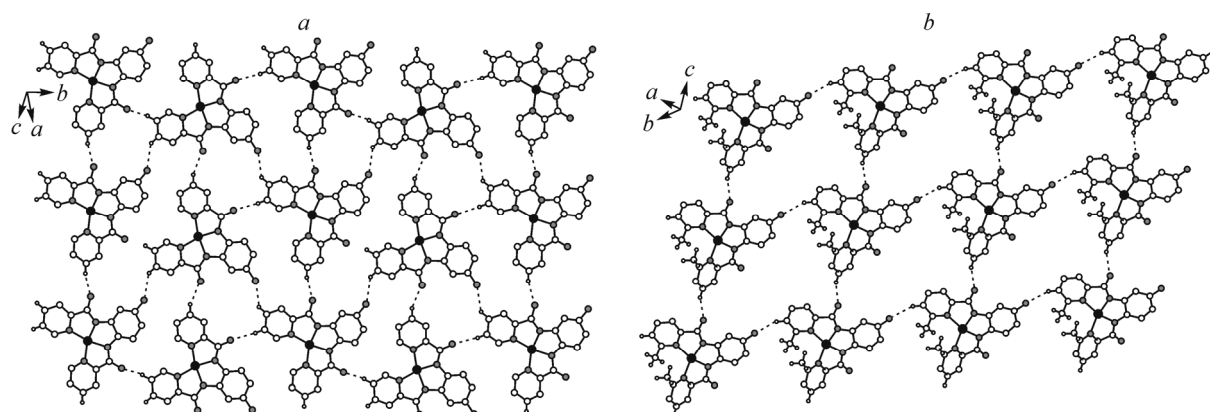


Fig. 3. Two-dimensional sheets built by C(pyridyl)—H...O and C(pyridyl)—H...F hydrogen bonds in compounds **4** (a) and **10** (b). H atoms not involved in intermolecular interactions have been omitted for clarity. The gray dotted lines represent C(methyl)—H...O interaction, and the open dotted lines represent C(methyl)—H...F interactions.

Hydrogen bond C...O or C...F lengths [angles]: for **4**, C16(pyridyl)—H16A...F1(1-x, -0.5+y, 0.5-z) 2.50(4) Å [138.43(1)°], C17(pyridyl)—H17A...O1(2-x, -0.5+y, 1.5-z) 2.269(3) Å [166.71(1)°], C3(pyridyl)—H3A...O2(1+x, y, 1+z) 2.36(4) Å [151.06(1)°]; for **10**, C17(pyridyl)—H17...F1(1+x, 1+y, z) 2.547(9) Å [156.14(3)°], C3(pyridyl)—H3...O1(x, y, -1+z) 2.323(6) Å [155.78(3)°]

same type of 2D sheets in both **4** and **10**. The presence of the 6-methyl group in the pyridyl 6'-positions does not effect hydrogen bonds. In compound **12** with 6-methyl group in the bpn^{2-} ligand, hydrogen bonds between methyl hydrogen atoms and carbonyl oxygen atoms generate a double chain (Fig. 4). In this case, the presence of methyl groups in the pyridyl 6'-positions is important for hydrogen bonds.

Voltammetric behavior. All the Ni(II) complexes showed reversible redox behavior with $i_{\text{pa}}/i_{\text{pc}} \approx 1$ and $\Delta E_{\text{p}} \approx 60$ mV, where i_{pa} is an anodic peak current, i_{pc} is a cathodic peak current, and ΔE_{p} is a peak separation of the cathodic and anodic peak potentials. Typical voltammograms are shown in Fig. 5 for **3** and **9**, the complexes differing only in R_1 : H for **3** and CH_3 for **9**. The reversible behavior implies that the reduced Ni(I) state of each complex is stable in the time scale of CV measurement. The formal potentials, E^0 , of the complexes were measured and calculated from $E^0 = (E_{\text{pc}} + E_{\text{pa}})/2$, where E_{pc} is a cathodic peak potential and E_{pa} is anodic peak potential. The formal potentials of the Ni complexes measured are listed in Table 3. The E^0 for the complex **3** was -1.82 V, and the E^0 for the complex **9** was -1.70 V. The complex **9**, which has methyl group as R_1 , has formal potential value

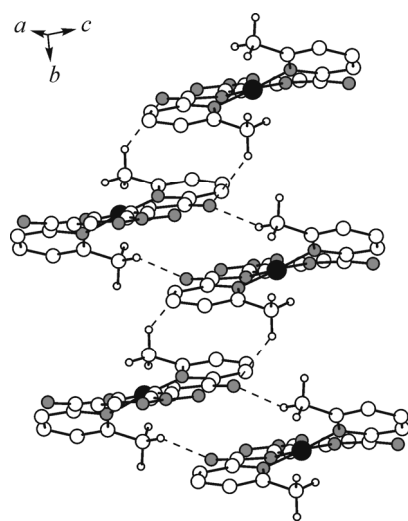
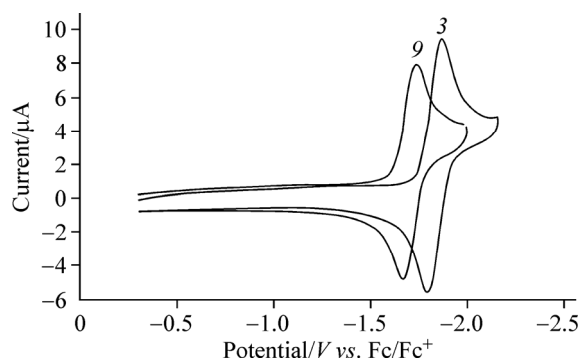


Fig. 4. A double chain built by C(methyl)—H...O hydrogen bonds in compound **12**. H atoms not involved in intermolecular interactions have been omitted for clarity. The open dotted lines represent C(methyl)—H...O interactions.

Hydrogen bond C...O lengths [angles]: C19(methyl)—H19A...O2(0.5+x, 0.5-y, -z) 2.451(2) Å [152.01(1)°], C20(methyl)—H20A...O2(0.5+x, 1.5-y, -z) 2.506(2) Å [135.13(1)°]

Fig. 5. CVs of **3** and **9** in 0.1 M TBABF₄/DMSO at 50 mV/s



120 mV more positive than **3**. It means that the introduction of CH₃ instead of H in R₁ position made the reduction of the complex easier. A similar behavior was observed for complexes **7** and **8** with easier reduction as compared to **1** and **2**, respectively. The introduction of the methyl group in other positions (X₁, X₂) caused almost no change in the potential (Table 3) indicating the electronic effect from the methyl group being insignificant. It is clear that the substitution effect of methyl group in R₁ position is more pronounced than in the positions of X₁ or X₂. Also, the electronic effect of the methyl group in R₁ position is not important since the potential shift is opposite if only the electron-donating character of the methyl group is counted. Instead, the distorted crystal structure produced by introducing 6-methyl group (**7**, **8** and **9**), which stabilize Ni(I) state, corresponds to the voltammetric results with a positive potential shift. It is a similar behavior to that we reported for the copper complexes [7]. As to the electronic effect caused by the groups X₁ and X₂, the potential shifts of the complexes reflect this electronic effect (Table 3). If the complexes **1** through **6** are compared, the formal potential shifts to more positive values due to increasing electron-withdrawing character of the substituents X₁ and X₂ when R₁ is the same. A similar electronic effect could be observed for the complexes **7** through **12**. In summary, the steric effect of R₁ and the electronic effects of X₁ and X₂ are major contributors to the voltammetric behavior of the Ni complexes.

Table 3

Formal potential data for Ni complexes in 0.1M TBABF₄/DMSO (V vs. Fc/Fc⁺)

Compound	X ₁	X ₂	R ₁	E° for Ni(II/I)
1	CH ₃	CH ₃	H	-1.85
2	H	CH ₃	H	-1.84
3	H	H	H	-1.82
4	H	F	H	-1.77
5	Cl	Cl	H	-1.70
6	H	NO ₂	H	-1.51
7	CH ₃	CH ₃	CH ₃	-1.72
8	H	CH ₃	CH ₃	-1.71
9	H	H	CH ₃	-1.71
10	H	F	CH ₃	-1.64
11	Cl	Cl	CH ₃	-1.58
12	H	NO ₂	CH ₃	-1.50

Financial support from Korea Ministry Environment "ET-Human resource development Project", the Korean Science & Engineering Foundation (R01-2008-000-20704-0 and 2009-0074066), the Converging Research Center Program through the National Research Foundation of Korea (NRF) funded by the Ministry of Education, Science and Technology (2009-0082832), and the SRC program of the Korea Science and Engineering Foundation (KOSEF) through the Center for Intelligent Nano-Bio Materials at Ewha Womans University (grant R11-2005-008-00000-0) is gratefully acknowledged.

REFERENCES

- Ni Z.-H., Kou H.-Z., Zhang L.F. *et al.* // J. Chem. Crystallogr. – 2006. – **36**. – P. 465, references therein.
- Afshar R.K., Eroy-Reveles A.A., Olmstead M.M., Mascharak P.K. // Inorg. Chem. – 2006. – **45**. – P. 10347.
- Fortney C.F., Shepherd R.E. // Inorg. Chem. Commun. – 2004. – **7**. – P. 1065.
- Lin J., Tu C., Lin H. *et al.* // Inorg. Chem. Commun. – 2003. – **6**. – P. 262.
- Vlahos A.T., Tolis E.I., Raptopoulou C.P. *et al.* // Inorg. Chem. – 2000. – **39**. – P. 2977.
- Lee S.H., Han H., Kwak H. *et al.* // Chem. Eur. J. – 2007. – **13**. – P. 9393.
- Lee D.N., Ryu J.Y., Kwak H. *et al.* // J. Mol. Struct. – 2008. – **885**. – P. 56.
- Stephens F.S., Vagg R.S. // Inorg. Chim. Acta. – 1986. – **120**. – P. 165.
- Lee D.H., Lee J.Y., Ryu J.Y. *et al.* // Bull. Korean Chem. Soc. – 2006. – **27**. – P. 1031.

10. Luan X.J., Wang Y.-Y., Li D.-S. *et al.* // *Angew. Chem. Int. Ed.* – 2005. – **44**. – P. 3864.
11. Ding B.-B., Weng Y.-Q., Mao Z.-W. *et al.* // *Inorg. Chem.* – 2005. – **44**. – P. 8836.
12. Angeloni A., Crawford P.C., Orpen A.G. *et al.* // *Chem. Eur. J.* – 2004. – **10**. – P. 3783.
13. Balamurugan V., Hundal M.S., Mukherjee R. // *Chem. Eur. J.* – 2004. – **10**. – P. 1683.
14. Wang Y., Yu J., Li Y. *et al.* // *Chem. Eur. J.* – 2003. – **9**. – P. 5048.
15. Braga D., Grepioni F., Desiraju G.R. // *Chem. Rev.* – 1998. – **98**. – P. 1375.
16. Janiak C., Scharmann T.G. // *Polyhedron.* – 2003. – **22**. – P. 1123.
17. Brammer L., Bruton E.A., Sherwood P. // *Cryst. Growth Des.* – 2001. – **1**. – P. 277.
18. Desiraju G.R. // *Acc. Chem. Res.* – 2002. – **35**. – P. 565.
19. Lee J.H., Kim H.J., Choi Y.W. *et al.* // *Polyhedron.* – 2007. – **26**. – P. 1388.
20. Lin J., Zhang J.Y., Xu Y. *et al.* // *Acta Crystallogr.* – 2001. – **C57**. – P. 192.
21. Jain S.L., Bhattacharyya P., Milton H.L. *et al.* // *Dalton Trans.* – 2004. – P. 862.
22. Lee S.J., Lee J.Y., Kim C. *et al.* // *Acta. Crystallogr.* – 2002. – **E58**. – P. m191.
23. Chapman R.S., Stephens F.S., Vagg R.S. // *Inorg. Chim. Acta.* – 1981. – **52**. – P. 161.
24. Nam S.H., Kwak H., Lee Y.M. *et al.* // *Anal. Sci.: X-Ray Struct. Analysis Online.* – 2006. – **22**. – P. x37.
25. Sheldrick G.M. SHELXS-97. A Program for Structure Determination. – University of Göttingen, Göttingen, Germany, 1990.
26. Sheldrick G.M. SHELXL-97. A Program for Structure Determination. – University of Göttingen, Göttingen, Germany, 1997.
27. Bruker, SHELXTL/PC. Version 6.12 for Windows XP. Bruker AXS Inc. – Madison, Wisconsin, USA, 2001.